



Affinities of organophosphate flame retardants to tumor suppressor gene p53: An integrated *in vitro* and *in silico* study



Fei Li^a, Lulu Cao^{a,d}, Xuehua Li^b, Na Li^c, Zijian Wang^c, Huifeng Wu^{a,*}

^a Key Laboratory of Coastal Zone Environmental Processes and Ecological Remediation, Yantai Institute of Coastal Zone Research (YIC), Chinese Academy of Sciences (CAS), Shandong Provincial Key Laboratory of Coastal Zone Environmental Processes, YICCAS, Yantai, Shandong 264003, PR China

^b Key Laboratory of Industrial Ecology and Environmental Engineering (MOE), School of Environmental Science and Technology, Dalian University of Technology, Linggong Road 2, Dalian 116024, PR China

^c State Key Laboratory of Drinking Water Science and Technology, Research Center for Eco-Environmental Sciences, Chinese Academy of Sciences, Beijing 100085, PR China

^d University of Chinese Academy of Sciences, Beijing 100049, PR China

HIGHLIGHTS

- The binding affinities of OPFRs for p53 DNA fragment were studied.
- The interaction of 9 OPFRs with p53 was explored by UV and fluorescence spectroscopy.
- The electrostatic potentials were found to be the dominant interactions.
- The QSAR had good robustness, predictive ability and mechanism interpretability.

ARTICLE INFO

Article history:

Received 23 September 2014

Received in revised form 1 December 2014

Accepted 7 December 2014

Available online 12 December 2014

Keywords:

Organophosphate flame retardants (OPFRs)

p53

Docking

Quantitative structure–activity relationship (QSAR)

Binding affinity

Partial least squares (PLS)

ABSTRACT

Health concerns have been raised in regards to the environmental impact of the more frequently used organophosphate flame retardants (OPFRs). In this study, the effects of two typical OPFRs (TCPP and TPHP) on p53 gene expression in human embryo liver L02 cells were determined by quantitative real-time PCR. To better understand the relationship between molecular structural features of OPFRs and binding affinities for the tumor suppressor genes p53, an integrated experimental and *in silico* approach was used. The interaction of 9 OPFRs with p53 DNA fragment under simulated physiological conditions (phosphate buffer solution of pH 7.40), was explored by UV absorption spectroscopy, fluorescence spectroscopy and molecular modeling method. The binding constants of 9 OPFRs with p53 DNA fragment were determined respectively, using ethidium bromide (EB) as fluorescence probe of DNA. From docking analysis, hydrogen bonding and hydrophobic interactions were found to be the dominant interactions. Based on the observed interactions, appropriate molecular structural parameters were adopted to develop a quantitative structure–activity relationship (QSAR) model. The binding affinities of OPFRs to p53 DNA fragment were related with molecular electrostatic potential. The developed QSAR model had good robustness, predictive ability and mechanism interpretability.

© 2014 Elsevier Ireland Ltd. All rights reserved.

Abbreviations: OPFRs, organophosphate flame retardants; TCEP, Tris(2-chloroethyl)phosphate; TCPP, Tris(2-chloroisopropyl)phosphate; TPrP, Tris(2-chloroisopropyl)phosphate; DnBP, di-*n*-butylphosphate; TEHP, Tris(2-ethylhexyl)phosphate; TPHP, triphenylphosphate; TEP, triethylphosphate; TMP, trimethylphosphate; TCrP, tricresyl phosphate; AD, applicability domain; E_{HOMO} , energy of the highest occupied molecular orbital; E_{LUMO} , energy of the lowest unoccupied molecular orbital; $\log K_{\text{OW}}$, logarithm of octanol/water partition coefficient; PLS, partial least squares; Q^2_{CUM} , the fraction of the total variation of the dependent variables that can be predicted by all the extracted components; QSAR, quantitative structure–activity relationship; R , determination coefficient; RMSE, root mean square error.

* Corresponding author. Tel.: +86 535 2109190; fax: +86 535 2109000.

E-mail address: hfwu@yic.ac.cn (H. Wu).

1. Introduction

Organophosphorus flame retardants (OPFRs) are considered as re-emerging pollutants because of their increased use after polybrominated diphenyl ethers (PBDEs) bans (Dishaw et al., 2011; van der Veen and de Boer, 2012). OPFRs can diffuse out into surroundings relatively easily by volatilization, leaching and/or abrasion since they are not covalently bound to host materials (Marklund et al., 2003; Reemtsma et al., 2008). OPFRs can be used as flame retardants and plasticizers in a wide variety

of applications, resulting in their ubiquitous occurrence in all environmental compartments including indoor dust (Marklund et al., 2003; Stapleton et al., 2009; Takigami et al., 2009), water (Bacaloni et al., 2008; Regnery and Puttmann, 2010), sediments (Garcia-Lopez et al., 2009), soils (David and Seiber, 1999) and even in the aquatic organisms and in human breast milk (Liu et al., 2012).

Compared with PBDEs, OPFRs have received little attention with regard to human exposure and potential toxicological effects. The chlorinated alkylphosphates such as Tris-(2-chloro-, 1-methyl-ethyl)-phosphate (TCPP) and Tris-(2-chloroethyl)-phosphate (TCEP) are mostly used as flame retardants in polyurethane foam, which are carcinogenic in animals (Andresen et al., 2004). Meeker and Stapleton (2010) reported that triphenyl phosphate (TPP) was associated with altered hormone levels and decreased semen quality in men, which was shown to be a potent human blood monocyte carboxylesterase inhibitor (Saboori et al., 1991). OPFRs could alter sex hormone balance through several mechanisms including alterations of steroidogenesis or estrogen metabolism (Liu et al., 2012). An avian *in vitro* screening study was recently conducted to aid in testing prioritization of 16 structurally diverse flame retardants (Porter et al., 2014). Considering their toxicity, more attention should be paid to human OPFRs exposure and the potential human health risk (Cao et al., 2012).

It is well-known that DNA is one of the most important biological molecules targeted by many small molecules, which can bind to DNA via covalent or non-covalent interactions. Many types of cancer can be partly attributed to gene mutations, initiate carcinogenesis and DNA damage induced by unwanted small molecules (Kashanian et al., 2012; Zhang et al., 2014). Søderlund et al. (1985) reported that Tris(1,3-dichloro-2-propyl) phosphate (Tris-CP), which was commercially available as flame retardants in synthetic fibers, plastics and urethane foams, was metabolized to products which were mutagenic for *Salmonella typhimurium* TA100 in the presence of liver microsomes from phenobarbital (PB)-pretreated rats and NADPH.

In recent years, the interaction between DNA and some chemicals including coumarins (Zhao et al., 2014), sodium saccharin (Zhang et al., 2014) and metolcarb (Li et al., 2014) have been reported. These studies have provided much useful information to elucidate the mechanism of binding interactions between chemicals and DNA. Therefore, exploring the complex formations of DNA with OPFRs is considered as an important step to provide valuable information about the genotoxicity and carcinogenicity of OPFRs.

p53 is a short-lived transcription factor that has been most extensively studied in its capacity to mediate innate tumor suppression (Vousden and Lane, 2007; Meek, 2009). In animal models, loss or mutation of p53 predisposes to a range of spontaneous and induced tumors (Iwakuma and Lozano, 2007), highlighting its protective role as a barrier to tumor development. It is reported that liver, breast, gastric and lung cancer are related with the p53 gene inactivation (Petitjean et al., 2007). Hence, it is of great importance to study the mechanism of gene damage caused by OPFRs and their structure–activity relationship (QSARs) for the interaction. Furthermore, molecular docking has become an integral part of many modern structure-based computational simulations of chemicals (Martinez et al., 2008). Combinational use of docking with QSAR can provide more information on the interaction between the ligand and the receptor (Li et al., 2010a,b, 2012).

In this study, the effects of TCPP and TPhP on p53 gene expression in human embryo liver L02 cells were determined by quantitative real-time PCR. The UV–vis absorption and fluorescence were employed to determine the binding mode of the OPFR–p53 DNA fragment interaction in physiological buffer

(pH 7.4). Moreover, molecular docking was performed to demonstrate the position and preferential docking sites of the representative OPFRs in p53 DNA fragment. Finally, the theory prediction QSAR model for the binding constants of OPFRs interacting with p53 DNA fragment is developed. The results may provide insight into the binding mechanism of OPFRs with p53 DNA fragment at the molecular level and potential hazards of the OPFRs.

2. Materials and methods

2.1. Instrument and reagent

The UV–vis absorption spectra were measured on a Shimadzu UV-2450 spectrophotometer equipped with a controlled cell holder matched with 1.0 cm quartz cells. The fluorescence spectral titrations were performed on a spectrofluorometer (model F-4500, Hitachi, Japan) with a DC-2006 thermostat bath (Ningbo Xinyi Ultrasonic Instrument Co., Ningbo, China). Appropriate blanks corresponding to the buffer were subtracted to correct the fluorescence background.

Tris(2-chloroethyl) phosphate (TCEP, 99.0%), Tris(2-chloroisopropyl) phosphate (TCPP, 99.5%), Tris(2-chloroisopropyl) phosphate (TPPr, 99.5%), di-*n*-butylphosphate (DnBP, 98.0%), Tris (2-ethylhexyl) phosphate (TEHP, 98.5%), triphenylphosphate (TPhP, 99.5%), triethylphosphate (TEP, 99.5%), trimethylphosphate (TMP, 99.5%) and tricresyl phosphate (TCrP, 98.5%) were purchased from J&K Chemical Ltd. (China). The ultrapure water from a Millipore Simplicity water purification system (Millipore, Molsheim, France) was used throughout the experiment. All solutions were adjusted to pH 7.4 with phosphate buffer solution (PBS).

2.2. Quantitative real-time PCR of p53 gene expression analysis

The human embryo liver L02 cells were kindly provided by Professor Sijin Liu in research center for eco-environmental sciences, Chinese academy of sciences and maintained in 1640 medium (Hyclone, USA), added with 10% (v/v) fetal bovine serum (FBS), 100 U/ml penicillin, and 100 µg/ml streptomycin, in a humidified atmosphere containing 5% CO₂ at 28 °C.

The L02 cells were exposed with low, media and high concentration (1, 10, 100 µM) of TCPP or TPhP for 24 h, respectively. Total RNA was isolated in TRIzol reagent (Invitrogen, Carlsbad, CA, USA) from the L02 cells following the manufacturer's directions. RT-PCR primers used to quantify the HPRT1 and p53 are F: TGACACTGGCAAAACAATGCA, R: GGTCCTTTTACCAGCAAGCT, F: TCTCCCCAGCCAAAGAAGAAA, R: TTCCAAGGCCTCATTACGCTC. The RT-PCR were implemented in a total volume of 20.0 µl containing 6.0 µl of 1:20 diluted cDNA, 0.4 µl of each primer, 10.0 µl of 2 × SYBR Green Master Mix and 3.2 µl of PCR-grade water in triplicate. The PCR program was started at 95 °C for 7 min, followed by 40 cycles for 10 s at 95 °C, 30 s at 60 °C. The last cycle was 95 °C for 35 s, 60 °C for 25 s. After that, data were analyzed with the ABI 7500 SDS software. The expression levels of p53 gene were calculated by the comparative CT (2^{-ΔΔC_T}) as previously described (Livak and Schmittgen, 2001).

2.3. The preparation of double-stranded DNA

The selected DNA segment sequence of p53 (5'-CCTCCTCCCAACTCC-3', 3'-GGAGGAGGGGTGAGG-5') was part of the p53 upstream promoter regions, which was used together with OPFRs in DNA-binding assay. Promoters contain specific DNA sequences and response elements that provide a secure initial binding site for RNA polymerase and for proteins called transcription factors that recruit RNA polymerase. It is

supposed that the normal transcription and translation will be interfered if OPFRs selectively binds to the promoter region of p53 gene.

The selected two complementary single-stranded p53 DNA segments were obtained from Shenggong Biotech (Shanghai, China). They were dissolved in PBS (pH 7.4, 500 μ M), which was kept in 85 °C for 12 min, annealing, and then slow cooling to room temperature, resulting in the double-stranded DNA solution (500 μ M). The purity of the double-stranded DNA was determined by the ratio of the absorbance at 260 nm to that at 280 nm. The current solution gave a ratio of A260/A280 > 1.8, suggesting that the double helix structure was formed from single-strand DNA (Santhiya et al., 2012).

2.4. OPFRs–p53 interaction studies by UV–vis and fluorescence spectra

To investigate the binding affinity between p53 DNA fragment and OPFRs, UV–vis and fluorescence spectra measurements were performed in pH 7.4 PBS at room temperature. The OPFRs were prepared as 0.1 M DMSO stock solution and was diluted by PBS for DNA binding studies (0, 2, 4, 8, 12, 16, 20 μ M). The p53 DNA fragment was diluted to 2 μ M and was added in different amounts of OPFRs. The concentration gradient of each OPFR for the determination is 0, 1, 2, 4, 6, 8, 10 μ M and that of p53 DNA fragment is 1 μ M. After the mixture was incubated for 60 min, the absorption spectra were performed from 190 to 350 nm.

In the competitive binding experiments, the fluorescence quenching efficiency of DNA–probe system by small molecule is usually used to determine its DNA binding affinity (Zhu et al., 2014). To further investigate on the mode of binding of each OPFRs, competitive ethidium bromide (EB) binding study was performed by fluorescence spectroscopic titration. Thus, to a solution of p53 DNA fragment (1 μ M) and EB (10 μ M) in PBS (pH 7.4), aliquots of a certain amount of a solution of OPFRs were added. The corresponding fluorescence spectra were recorded with excitation at 480 nm and emission at 500–800 nm.

According to the classical Sterne–Volmer equation:

$$\frac{F_0}{F} = 1 + K_{SV}[Q] \quad (1)$$

where F_0 and F are the fluorescence intensities of DNA in the absence and presence of OPFRs complex, respectively. Also K_{SV} is the Stern–Volmer quenching constant and $[Q]$ is the concentration of the quencher.

The binding constant (K_b) and the number of binding sites (n) for OPFRs–p53 system can be determined by the following equation (Janishidi et al., 2014).

$$\log[(F_0 - F)] = \log K_b + n \log [Q] \quad (2)$$

where K_b and n are the binding constant and the number of binding sites in base pairs, respectively.

2.5. Molecular modeling

The crystal structure of the p53 DNA fragment was generated from the web site (<http://structure.usc.edu/make-na/server.html>). The following molecular docking studies were implemented with the software package CDocker, which has been incorporated into Discovery Studio 2.5 (Accelrys Software Inc.) through the Dock Ligands protocol. CDocker is an implementation of the docking tool based on the CHARMM force field that has been proven to be viable (Wu et al., 2003). In CDocker, 10 random ligand conformations are generated. The conformations are further refined by grid-based simulated annealing in the binding site, which makes the results accurate. In addition, the electrostatic potentials of the p53 DNA fragment were calculated by the

electrostatic protocol that had been incorporated into Discovery Studio 2.5. From the docking analysis, insights into the interactions between the OPFRs and the p53 DNA fragment were gained.

2.6. Mechanism consideration and molecular structural parameters selection

It was hypothesized that the binding affinities between OPFRs and p53 DNA fragment depended on the following two processes: (a) the penetration of OPFRs through bio-membrane and reaching the target site of action, and (b) the interactions between the OPFRs and p53 DNA fragment. Thus, theoretical parameters were computed and selected to characterize the processes. For example, the logarithm of octanol/water partition coefficient ($\log K_{OW}$) was purposely selected to describe the partition process, which was obtained from Reemtsma et al. (2008). The parameters molecular volume (V), the average molecular polarizability (α) and the polarizability term (π_i) (Famini and Wilson, 1999) were also selected to partly describe the partition since they correlated with $\log K_{OW}$ (Nguyen et al., 2005). The energy of the highest occupied molecular orbital (E_{HOMO}) and the energy of the lowest unoccupied molecular orbital (E_{LUMO}) were selected to describe the ability of accepting proton and donating proton, respectively, which had been used to predict the binding affinities of compounds (Gao et al., 1999; Hu and Aizawa, 2003). The most positive hydrogen atom in the molecule (qH^+), the most negative formal charge in the molecule (q^-), electrophilicity index (ω), the most positive and most negative values of the molecular surface potential ($V_{s,max}$, $V_{s,min}$), the averages of the positive and negative potentials on the molecular surface (\bar{V}_s^+ , \bar{V}_s^-), the average deviation of surface potential (Π) and the balance parameter of surface potential (τ) were purposely selected to describe the intermolecular electrostatic interactions between the OPFRs and the receptor p53 DNA fragment. These quantum molecular descriptors were computed by Gaussian 09 programs (Frisch et al., 2009). Initial geometries of the compounds were optimized by semi-empirical method PM3, then optimized at the hybrid Hartree–Fock density functional theory B3LYP/6-31G (d, p) level. Solvent effects (water) were taken into consideration implicitly, including the integral equation formulation of the polarized continuum model (IEFPCM). The frequency analysis was performed on the optimized geometries to ensure that the systems had no imaginary vibration frequencies. More details for these descriptors were shown in Table S1. Additionally, DRAGON software was also employed to calculate molecular structural descriptors. 1481 descriptors were computed, and then those with constant were discarded.

2.7. Model development and validation

Partial least squares (PLS) regression was performed for the model development as PLS can analyze data with strongly collinear, noisy and numerous predictor variables. Simca-S (Version 6.0, Umetri AB & Erisoft AB) was employed for the PLS analysis. The conditions for the computation were: cross-validation rounds = 7, maximum iteration = 200, missing data tolerance = 50%, and significance level limit = 0.05. Within Simca, the number of significant PLS components (A , model dimensionality) is determined by cross-validation. With cross-validation, observations are kept out of the model development, and then the response values (Y) for the excluded observations are predicted by the model and compared with the actual values. This procedure is repeated several times until every observation has been kept out once and only once. Cross-validation simulates how well a model predicts new data, and gives a statistical Q^2_{CUM} (the fraction of the total variation of the dependent variables that can be predicted by all the extracted

components) for model. The PLS analysis was performed repeatedly so as to eliminate redundant molecular structural parameters, as done in our previous studies (Li et al., 2010a,b, 2012).

3. Results and discussion

3.1. Effect of OPFRs on p53 genes expression in L02 cells

The variation profiles of p53 mRNA expression in human embryo liver L02 cells were shown in Fig. 1. The p53 mRNA level was significantly increased in L02 cells treated with TCPP and TPhP in a dose-dependent manner, indicating that apoptosis induced by OPFRs depended on the induction and activation of p53. The central transcription factor p53 governs the signals arising from DNA adducts. The p53 pathway is central in the response to DNA damage (Clewell et al., 2014). Hence, the binding interaction between OPFRs and p53 DNA segments was studied as following.

3.2. UV absorption spectroscopy studies

The DNA binding properties of 9 OPFRs with p53 DNA fragment were investigated by UV–vis spectra in PBS (0.1 M, pH 7.4) at 25 °C. As shown in Fig. 2 and Table 1, in the presence of increasing concentration of OPFRs, the absorption intensities of p53 DNA segment enhanced in high hyperchromities, respectively, and the maximum absorption (λ_{\max}) showed blue shift (1.0–4.0 nm). The observed spectral changes (hypsochromism and blue shift) implied that there were interactions between OPFRs and p53 DNA fragment, which may damage the structure of DNA or insert into the base pairs of DNA as DNA-intercalating agents.

To further investigate on the mode of binding of each OPFR, the fluorescence properties were performed to investigate the interactions between 9 OPFRs and p53 DNA segment in PBS (0.1 M, pH 7.4) at 25 °C. As DNA itself has no fluorescence, EB is expected to help investigate the interaction of OPFRs with p53 DNA segment as a probe. EB is a typical mutagenic intercalating dye for DNA and it has been studied for many years. The significant quenching of the DNA–EB fluorescence suggests that the complex can compete for DNA-binding sites with EB and displace EB from the DNA–EB system, which is usually characteristic of the intercalative interaction of compounds with DNA (Anjomshoa et al., 2014; Tian et al., 2014).

As shown in Fig. 3, the fluorescent intensity of EB–DNA is remarkably quenched upon adding the 9 OPFRs and a dose–response

phenomenon is observed, which represents the replacement of EB by these complexes.

From the linear plot of $\log [(F_0 - F)/F]$ versus $\log [Q]$, K_b and n were calculated and listed in Tables 1 and 2. Among them, TPhP had the highest binding constant, which suggested that the OPFRs with phenyl group have stronger binding properties with p53 DNA segment than that with chlorine or hydrocarbonyl substituent groups. The exact interaction between DNA and 9 OPFRs can be more complicated since the linear relationship is not well presented and there may exist other interactions between OPFRs and DNA.

3.3. Docking analysis

To embody above experimental results and further understand the mode of interaction, molecular docking studies were performed to get valuable information. Molecular modeling has played an important role in studying the interaction of small molecules with biomacromolecules (Li et al., 2010a,b, 2012). Fig. 4 shows the docking view of 3 representative OPFRs (Tris(2-chloroethyl) phosphate, tri-*n*-propylphosphate and tri-phenylphosphate) in the binding site of DNA. Hydrogen-bondings are observed to be characteristic interactions. Hydrogen bond was the main source to maintain the stability of the system of OPFRs with DNA: (a) H-bonds formed between the oxygen of phosphorus oxygen double bond and the phenyl of thymine; (b) H-bonds between the oxygen of alkyl oxygen bond and the hydrogen of thymine.

Acting as an 'anchor', the hydrogen-bonding intensely determines the 3D space position of the OPFRs in the binding pocket, and facilitates the hydrophobic interaction of the OPFRs with adenine (A), thymine (T), cytosine (C) and guanine (G), as shown in Fig. 4. Additionally, there are also π - π interactions between the phenyl of TPhP and cytosine (C) or thymine (T).

The molecular surface potential indicates the charge distribution in a molecule, which gauge the basicity and nucleophilicity of a molecule. As shown in Fig. S1, the binding site has positive potentials, from which it can also be concluded that the negative potentials of the OPFR molecules facilitate them to bind with DNA. Therefore, the results obtained from the above molecular modeling demonstrated that there are two interaction modes between OPFRs and p53 DNA segment, the electrostatic binding mode and the intercalation binding mode, which consists of the experimental results from the spectroscopic studies.

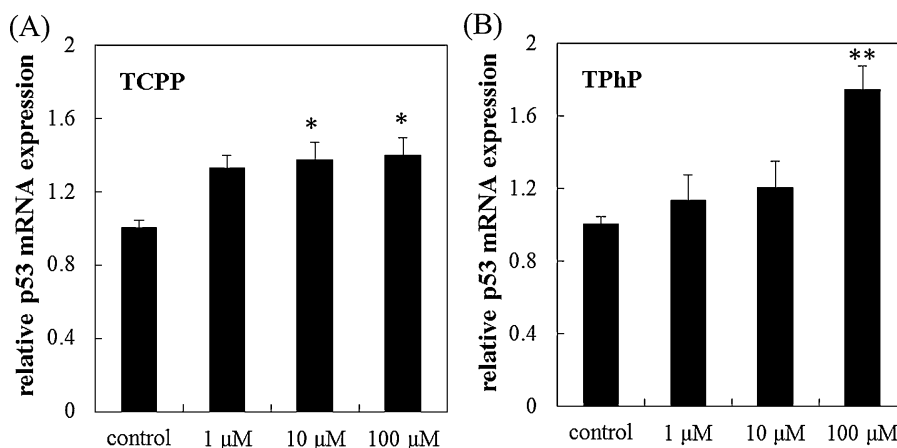


Fig. 1. Induction of expression of p53 in the L02 cells after exposure to different concentrations of TCPP (A) and TPP (B), respectively. (A) Total RNA was isolated and quantitative RT-PCR carried out for the detection of levels of p53. Data were normalized to expression of the HPRT1 housekeeping gene. Results are means \pm S.D. of two independent experiments each carried out in triplicate. * $p < 0.05$, ** $p < 0.01$.

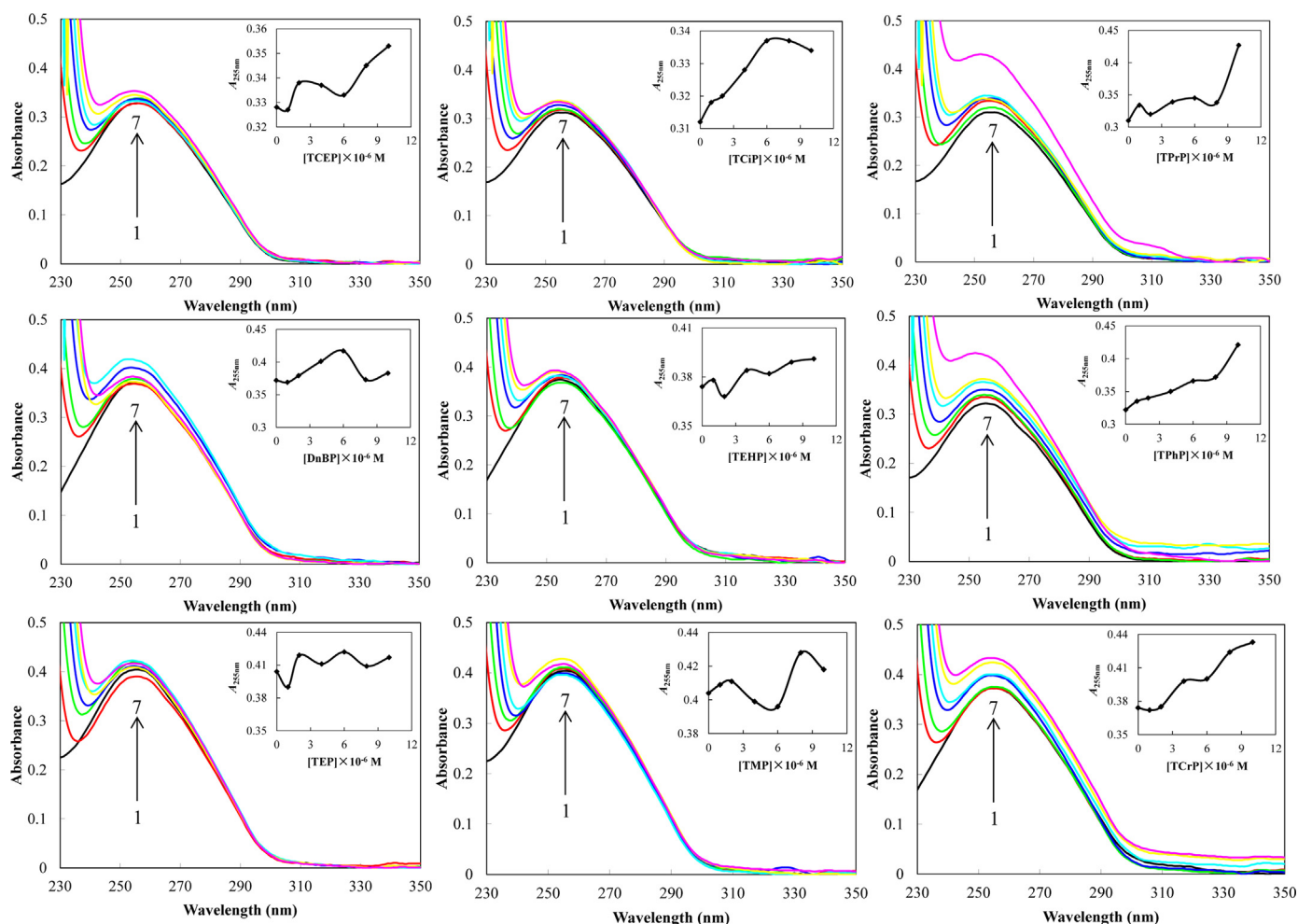


Fig. 2. UV-vis spectral changes of the p53 gene segment at the concentration of 1 μM upon addition of 9 OPFRs compounds in PBS (0.1 M, pH 7.4) at 25 $^{\circ}\text{C}$. $c(\text{OPFRs}) = 0, 1, 2, 4, 6, 8$ and 10 μM , for curves 1–7, respectively. Inset: the fitting plots for OPFRs with p53 obtained at the maximum absorption.

3.4. Development and validation of the QSAR model for the $\log K_b$

Forward stepwise regression was adopted to screen significant molecular descriptors. Finally, 7 molecular descriptors were selected as the predictive variables for model development, which are listed in Table 2.

PLS analysis with the $\log K_b$ as the dependent variable and the molecular structural parameters as predictor variables resulted in the following optimal QSAR model: $\log K_b = -1.79 \times 10^{-1} + 3.75 N + 4.38 \bar{V}_s^- + 2.70 \times 10^{-1} \text{MATS}_{8e}$, $n = 9$, $A = 2$, $R^2 = 0.924$, $Q^2_{\text{CUM}} = 0.890$, $\text{SE} = 0.670$, $p < 0.001$ where p is the significance level.

Table 1

Photometric properties of the 9 OPFRs with p53 gene segment investigated by UV-vis spectra and binding constants (K_b) by fluorescence spectra.

No.	Compounds	Hypsochromic shift (nm)	Hyperchromicity ^a (%)	K_b^b (M^{-1})
1	TCEP	1.5 (256–254.5)	7.6	4.0×10^2
2	TCEPP	1.0 (255–254)	7.1	9.8×10^1
3	TPrP	4.0 (256–252)	39.0	2.0×10^2
4	DnBP	2.0 (255–253)	13.6	3.4×10^1
5	TEHP	2.0 (255–253)	5.1	1.4×10^3
6	TPhP	3.5 (255.5–252)	32.0	1.2×10^3
7	TEP	1.5 (255.5–254)	8.2	4.8×10^0
8	TMP	1.0 (255.5–254.5)	5.9	9.1×10^1
9	TCrP	1.0 (255–254)	18.7	1.3×10^2

^a Obtained at k_{max} .

^b Binding constants (K) by fluorescence spectra.

The predicted $\log K_b$ values and residuals for compounds are listed in Table 3. The R^2 value of the QSAR model was 0.924, indicating a better goodness-of-fit of the model. Q^2_{CUM} of the QSAR is as high as 0.890, implying good robustness of the model. The differences between R^2 and Q^2_{CUM} (0.034) did not exceed 0.3, indicating no over-fitting in the model (Golbraikh and Tropsha, 2002). The predicted $\log K_b$ values were consistent with the observed values. In summary, the developed QSAR model shows satisfactory performance which can illuminate the mechanism of interaction between OPFRs and p53 DNA segment and can be used to predict the $\log K_b$ values of other OPFRs.

3.5. Mechanistic implications of the developed QSAR model

Values of the variable importance in the projection (VIP) and PLS weights (W^*) are listed in Table 4. The W^* values can be used to estimate how the predictor variables and the response variables combine in the projections (PLS components), and how they relate to each other.

The established PLS model extracted two PLS component loaded primarily on 3 predictor variables, the number of binding site (N), \bar{V}_s^- , and MATS_{8e} . (N remarkably governs $\log K_b$, as indicated by its VIP, the largest among all the predictor variables. \bar{V}_s^- itself also has a negative value, and stands for the average of the negative potentials on the molecular surface. The electrostatic potential analysis showed that the binding site preferred to bind with the negative potentials on the molecules (Fig. S1). Hence, it is

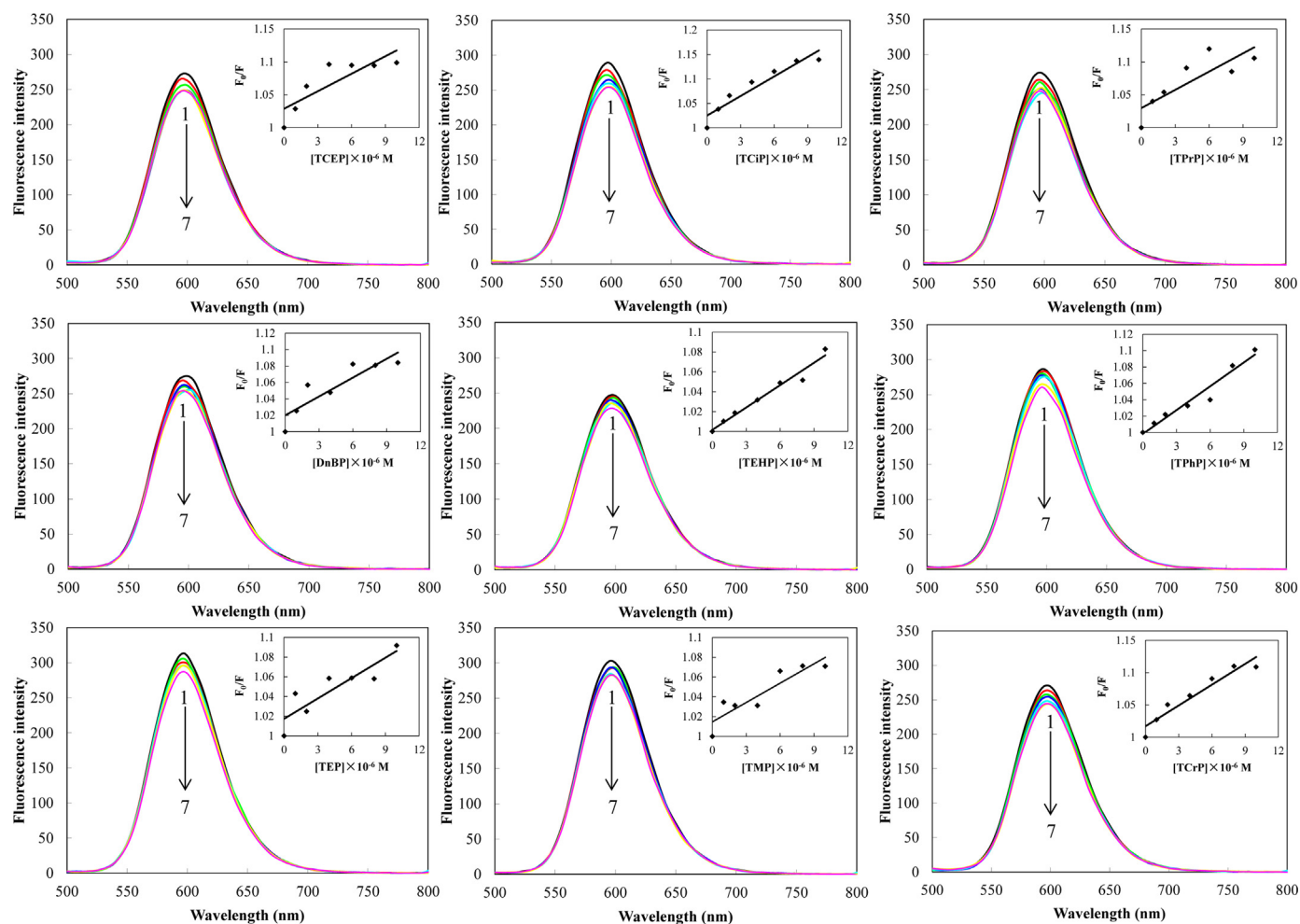


Fig. 3. Fluorescence spectral changes of p53 gene segment at the concentration of 1 μM upon addition of 9 OPFRs in PBS (0.1 M, pH 7.4) at 25 $^{\circ}\text{C}$. $c(\text{OPFRs}) = 0, 1, 2, 4, 6, 8$ and 10 μM , for curves 1–7, respectively. Both excitation and emission slit widths were 10.0 nm. The inset figure shows a plot of $[F_0/F]$ versus $[Q]$ and the arrow indicates the intensity changes on increasing the concentration of each complex.

reasonable that in the developed PLS model $\log K_b$ increases with decreasing \bar{V}_s^- values. The positive coefficient of \bar{V}_s^- in the current QSAR model indicated that OPFRs molecules with stronger negative molecular electrostatic potential were more easy to interact with DNA.

The second PLS components also extract 2 descriptors, N and MATS_{8e} . MATS_{8e} is a 2D autocorrelation descriptor that is weighted by atomic Sanderson electronegativities (Roy and Kadam, 2006). The coefficient of MATS_{8e} in the current QSAR model indicates the positive correlation between MATS_{8e} and $\log K_b$. In general, the

Table 2
Molecular descriptors in the developed QSAR model.

No.	Name	$\log K_{ow}^a$	Binding site (N)	$V_{s,max}^b$	$\bar{V}_s^-^c$	Π^d	E_{HOMO}^e	MATS_{8e}^f
1	TCEP	1.44	0.684	138.04	−0.005	0.070	−0.307	0.000
2	TCP	2.59	0.566	144.74	−0.008	0.052	−0.281	0.119
3	TPrP	1.87	0.623	168.51	−0.016	0.054	−0.302	0.138
4	DnBP	2.29	0.458	66.897	−0.013	0.051	−0.309	0.121
5	TEHP	9.49	0.985	125.56	−0.008	0.052	−0.301	−0.057
7	TPhP	4.59	0.839	133.00	−0.011	0.069	−0.262	0.081
8	TEP	0.80	0.366	66.99	−0.147	0.057	−0.306	0.273
9	TMP	0.30	0.482	219.94	−0.017	0.060	−0.310	0.000
10	TCrP	5.11	0.609	110.28	−0.010	0.058	−0.250	−0.368

^a $\log K_{ow}$ is the logarithm of octanol/water partition coefficient.

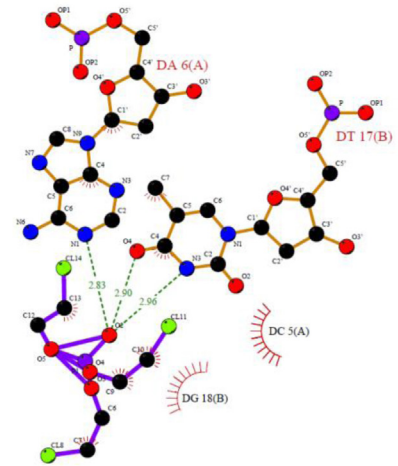
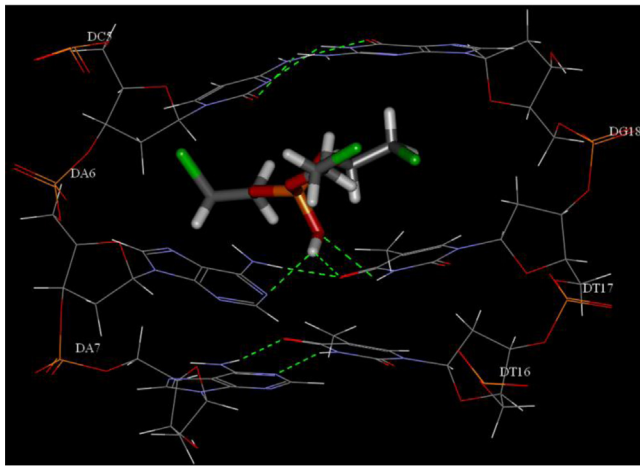
^b $V_{s,max}$ is the most positive values of the molecular surface potential.

^c is the averages of the negative potentials on the molecular surface.

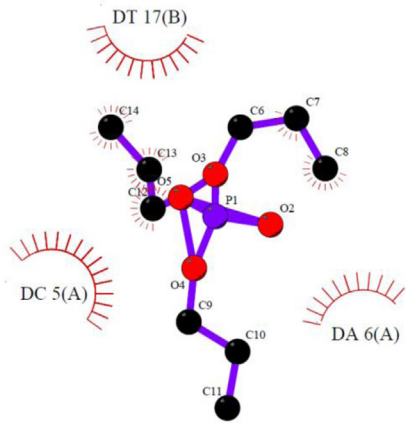
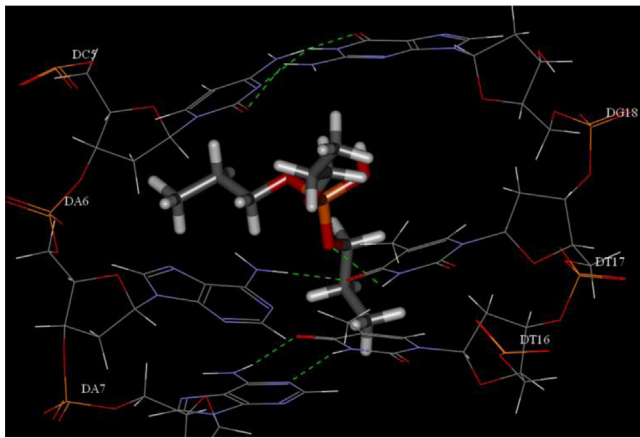
^d Π is the average deviation of surface potential.

^e E_{HOMO} is the energy of the highest occupied molecular orbital.

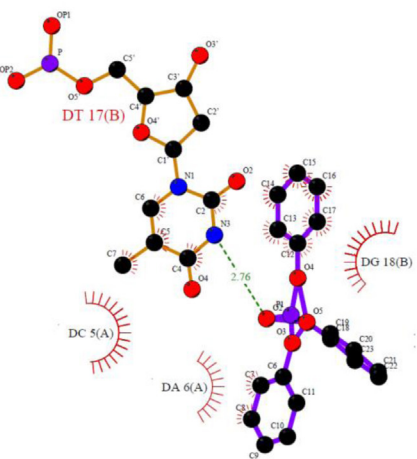
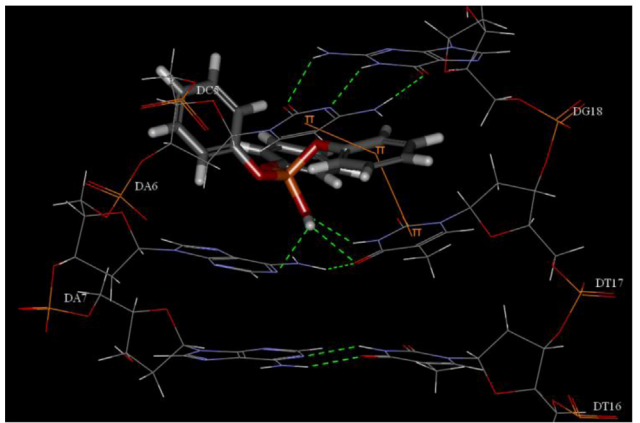
^f MATS_{8e} is a 2D autocorrelation descriptor that is weighted by atomic Sanderson electronegativities.



(a) Tris(2-chloroethyl)phosphate



(b) Tri-n-propylphosphate



(c) Triphenylphosphate

Fig. 4. Hydrogen bondings (left) and hydrophobic interactions (right) between Tris(2-chloroethyl) phosphate, tri-n-propylphosphate and triphenylphosphate in the binding site of DNA.

Table 3

Logarithm of the observed and predicted binding constant ($\log K_b$) of the considered compounds.

No.	Compounds	$\log K_b$		
		Observed	Predicted	Residuals
1	TCEP	2.619	2.361	0.258
2	T CPP	2.009	1.939	0.070
3	TPrP	2.321	2.122	0.199
4	DnBP	1.117	1.513	-0.396
5	TEHP	3.163	3.460	-0.297
6	TPhP	3.083	2.938	0.144
7	TEP	0.693	0.625	0.068
8	TMP	1.345	1.552	-0.206
9	TCrP	2.121	1.960	0.161

Table 4

VIP values and PLS weights for the optimal PLS model.

	VIP	$W^*c[1]$	$W^*c[2]$
N^a	1.331	0.794	0.743
\bar{V}_s^{-b}	0.885	0.523	-0.296
$MATS_{ge}^c$	0.667	-0.309	0.645

^a N is the number of binding site.

^b is the averages of the negative potentials on the molecular surface.

^c $MATS_{ge}$ is a 2D autocorrelation descriptor that is weighted by atomic Sanderson electronegativities.

current QSAR model indicated that the $\log K_b$ value was related to the number of binding site and electrostatic potential.

4. Conclusion

In this study, OPFRs could induce the expression of p53 mRNA. The interaction of OPFRs with p53 DNA segment was studied by UV absorption, fluorescence spectroscopy, molecular docking and QSAR. There were intercalation and electrostatic interaction between OPFRs and p53 DNA segment. Molecular docking studies provided direct evidence for the interaction and supported the experimental results. The OPFRs with stronger negative molecular electrostatic potential tended to bind with p53 DNA segment easily. The developed QSAR model had good robustness, predictive ability, and mechanism interpretability, which further advanced our knowledge of the interaction of OPFRs with p53 DNA segment and could be useful in assessing the toxicologic effects of OPFRs.

Conflict of interest

The authors declare that there are no conflicts of interest.

Transparency document

The Transparency document associated with this article can be found in the online version.

Acknowledgments

This research was supported by the National Natural Science Foundation of China (21107136, 21437006) and the International Foundation for Science (F/5230-1).

Appendix A. Supplementary data

Supplementary data associated with this article can be found, in the online version, at <http://dx.doi.org/10.1016/j.toxlet.2014.12.006>.

References

- Andresen, J.A., Grundmann, A., Bester, K., 2004. Organophosphorus flame retardants and plasticisers in surface waters. *Sci. Total Environ.* 332, 155–166.
- Anjomshoa, M., Fatemi, S.J., Mahani, M.T., Hadadzadeh, H., 2014. DNA- and BSA-binding studies and anticancer activity against human breast cancer cells (MCF-7) of the zinc(II) complex coordinated by 5,6-diphenyl-3-(2-pyridyl)-1,2,4-triazine. *Spectrochim. Acta A* 127, 511–520.
- Bacaloni, A., Cucci, F., Guarino, C., Nazzari, M., Samperi, R., Lagana, A., 2008. Occurrence of organophosphorus flame retardant and plasticizers in three volcanic lakes of Central Italy. *Environ. Sci. Technol.* 42, 1898–1903.
- Cao, S.X., Zeng, X.Y., Song, H., Li, H.R., Yu, Z.Q., Sheng, G.Y., Fu, J.M., 2012. Levels and distributions of organophosphate flame retardants and plasticizers in sediment from Taihu Lake, China. *Environ. Toxicol. Chem.* 31, 1478–1484.
- Clewell, R.A., Sun, B., Adeleye, Y., Carmichael, P., Efremenko, A., McMullen, P.D., Pendse, S., Trask, O.J., White, A., Andersen, M.E., 2014. Profiling dose-dependent activation of p53-mediated signaling pathways by chemicals with distinct mechanisms of DNA damage. *Toxicol. Sci.* 142, 56–73.
- David, M.D., Seiber, J.N., 1999. Analysis of organophosphate hydraulic fluids in US Air Force base soils. *Arch. Environ. Contam. Toxicol.* 36, 235–241.
- Dishaw, L.V., Powers, C.M., Ryde, I.T., Roberts, S.C., Seidler, F.J., Slotkin, T.A., Stapleton, H.M., 2011. Is the PentaBDE replacement, tris (1,3-dichloropropyl) phosphate (TDCPP), a developmental neurotoxicant? Studies in PC12 cells. *Toxicol. Appl. Pharmacol.* 256, 281–289.
- Famini, G.R., Wilson, L.Y., 1999. Using theoretical descriptors in linear free energy relationships: characterizing several polarity, acid and basicity scales. *J. Phys. Org. Chem.* 12, 645–653.
- Frisch, M.J., Trucks, G.W., Schlegel, H.B., Scuseria, G.E., Robb, M.A., Cheeseman, J.R., Scalmani, G., Barone, V., Mennucci, B., Petersson, G.A., Nakatsuji, H., Caricato, M., Li, X., Hratchian, H.P., Izmaylov, A.F., Bloino, J., Zheng, G., Sonnenberg, J.L., Hada, M., Ehara, M., Toyota, K., Fukuda, R., Hasegawa, J., Ishida, M., Nakajima, T., Honda, Y., Kitao, O., Nakai, H., Vreven, T., Montgomery Jr., J.A., Peralta, J.E., Ogliaro, F., Bearpark, M., Heyd, J.J., Brothers, E., Kudin, K.N., Staroverov, V.N., Kobayashi, R., Normand, J., Raghavachari, K., Rendell, A., Burant, J.C., Iyengar, S.S., Tomasi, J., Cossi, M., Rega, N.J., Millam, Klene, M., Knox, J.E., Cross, J.B., Bakken, V., Adamo, C., Jaramillo, J., Gomperts, R.E., Stratmann, O., Yazyev, A.J., Austin, R., Cammi, C., Pomelli, J.W., Ochterski, R., Martin, R.L., Morokuma, K., Zakrzewski, V. G., Voth, G.A., Salvador, P., Dannenberg, J.J., Dapprich, S., Daniels, A.D., Farkas, O., Foresman, J.B., Ortiz, J.V., Cioslowski, J., Fox, D.J., 2009. Gaussian 09, Revision A.1. Gaussian, Inc., Wallingford CT.
- Gao, H., Katzenellenbogen, J.A., Garg, R., Hansch, C., 1999. Comparative QSAR analysis of estrogen receptor ligands. *Chem. Rev.* 99, 723–744.
- García-Lopez, M., Rodriguez, I., Cela, R., 2009. Pressurized liquid extraction of organophosphate triesters from sediment samples using aqueous solutions. *J. Chromatogr. A* 1216, 6986–6993.
- Golbraikh, A., Tropsha, A., 2002. Beware of q^2 ! *J. Mol. Graph. Model.* 20, 269–276.
- Hu, J.Y., Aizawa, T., 2003. Quantitative structure-activity relationships for estrogen receptor binding affinity of phenolic chemicals. *Water Res.* 37, 1213–1222.
- Iwakuma, T., Lozano, G., 2007. Crippling p53 activities via knock-in mutations in mouse models. *Oncogene* 26, 2177–2184.
- Janishidi, M., Yousefi, R., Nabavizadeh, S.M., Rashidi, M., Haghighi, M.G., Niazi, A., Moosavi-Movahedi, A.A., 2014. Anticancer activity and DNA-binding properties of novel cationic Pt(II) complexes. *Int. J. Biol. Macromol.* 66, 86–96.
- Kashanian, S., Shariati, Z., Roshanfekar, H., Ghobadi, S., 2012. DNA binding studies of 3,5,6-trichloro-2-pyridinol pesticide metabolite. *DNA Cell Biol.* 31, 1341–1348.
- Li, F., Li, X.H., Shao, J.P., Chi, P., Chen, J.W., Wang, Z.J., 2010a. Estrogenic activity of anthraquinone derivatives: *in vitro* and *in silico* studies. *Chem. Res. Toxicol.* 23, 1349–1355.
- Li, F., Xie, Q., Li, X.H., Li, N., Chi, P., Chen, J.W., Wang, Z.J., Hao, C., 2010b. Hormone activity of hydroxylated polybrominated diphenyl ethers on human thyroid receptor β : *in vitro* and *in silico* investigations. *Environ. Health Perspect.* 118, 602–606.
- Li, F., Wu, H.F., Li, L.Z., Li, X.H., Zhao, J.M., Peijnenburg, W.J.G.M., 2012. Docking and QSAR study on the binding interactions between polycyclic aromatic hydrocarbons and estrogen receptor. *Ecotoxicol. Environ. Saf.* 80, 273–279.
- Li, Y., Zhang, G.W., Pan, J.H., Zhang, Y., 2014. Determination of metolcarb binding to DNA by spectroscopic and chemometrics methods with the use of acridine orange as a probe. *Sens. Actuators B* 191, 464–472.
- Liu, X., Ji, K., Choi, K., 2012. Endocrine disruption potentials of organophosphate flame retardants and related mechanisms in H295R and MVLN cell lines and in zebrafish. *Aquat. Toxicol.* 114, 173–181.
- Livak, K.J., Schmittgen, T.D., 2001. Analysis of relative gene expression data using real-time quantitative PCR and the $2^{-\Delta\Delta C_T}$ method. *Methods* 25, 402–408.
- Marklund, A., Andersson, B., Haglund, P., 2003. Screening of organophosphorus compounds and their distribution in various indoor environments. *Chemosphere* 53, 1137–1146.
- Martinez, L., Polikarpov, I., Skaf, M.S., 2008. Only subtle protein conformational adaptations are required for ligand binding to thyroid hormone receptors: simulations using a novel multipoint steered molecular dynamics approach. *J. Phys. Chem. B* 112, 10741–10751.
- Meek, D.W., 2009. Tumour suppression by p53: a role for the DNA damage response? *Nat. Rev. Cancer* 9, 714–723.
- Meeker, J.D., Stapleton, H.M., 2010. House dust concentrations of organophosphate flame retardants in relation to hormone levels and semen quality parameters. *Environ. Health Perspect.* 118, 318–323.

- Nguyen, T.H., Goss, K.U., Ball, W.P., 2005. Polyparameter linear free energy relationships for estimating the equilibrium partition of organic compounds between water and the natural organic matter in soils and sediments. *Environ. Sci. Technol.* 39, 913–924.
- Petitjean, A., Mathe, E., Kato, S., Ishioka, C., Tavtigan, S.V., Hainaut, P., Olivier, M., 2007. Impact of mutant p53 functional properties on TP53 mutation patterns and tumor phenotype: lessons from recent developments in the IARC TP53 database. *Hum. Mutat.* 28, 622–629.
- Porter, E., Crump, D., Egloff, C., Chiu, S., Kennedy, S.W., 2014. Use of an avian hepatocyte assay and the avian toxchip polymerase chain reaction array for testing prioritization of 16 organic flame retardants. *Environ. Toxicol. Chem.* 33, 573–582.
- Reemtsma, T., Quintana, J.B., Rodil, R., Garcia-Lopez, M., Rodriguez, I., 2008. Organophosphorus flame retardants and plasticizers in water and air I: occurrence and fate. *TrAC Trends Anal. Chem.* 27, 727–737.
- Regnery, J., Puttmann, W., 2010. Occurrence and fate of organophosphorus flame retardants and plasticizers in urban and remote surface waters in Germany. *Water Res.* 44, 4097–4104.
- Roy, N., Kadam, R.U., 2006. Cluster analysis and two-dimensional quantitative structure-activity relationship (2D-QSAR) of *Pseudomonas aeruginosa* deacetylase LpxC inhibitors. *Bioorg. Med. Chem. Lett.* 16, 5136–5143.
- Saboori, A.M., Lang, D.M., Newcombe, D.S., 1991. Structural requirements for the inhibition of human monocyte carboxylesterase by organophosphorus compounds. *Chem. Biol. Interact.* 80, 327–338.
- Santhiya, D., Dias, R.S., Dutta, S., Das, P.K., Miguel, M.G., Lindman, B., Maiti, S., 2012. Kinetic studies of amino acid-based surfactant binding to DNA. *J. Phys. Chem. B* 116, 5831–5837.
- Søderlund, E.J., Dybing, E., Holme, J.A., Hongslo, J.K., Rivedal, E., Sanner, T., Nelson, S.D., 1985. Comparative genotoxicity and nephrotoxicity studies of the two halogenated flame retardants tris(1,3-dichloro-2-propyl) phosphate and tris(2,3-dibromopropyl) phosphate. *Acta Pharmacol. Toxicol.* 56, 20–29.
- Stapleton, H.M., Klosterhaus, S., Eagle, S., Fuh, J., Meeker, J.D., Blum, A., Webster, T.F., 2009. Detection of organophosphate flame retardants in furniture foam and US house dust. *Environ. Sci. Technol.* 43, 7490–7495.
- Takigami, H., Suzuki, G., Hirai, Y., Ishikawa, Y., Sunami, M., Sakai, S., 2009. Flame retardants in indoor dust and air of a hotel in Japan. *Environ. Int.* 35, 688–693.
- Tian, Z.Y., Zhao, Z.H., Zang, F.L., Wang, Y.Q., Wang, C.J., 2014. Spectroscopic study on the interaction between naphthalimide-polyamine conjugates and DNA. *J. Photochem. Photobiol. B* 138, 202–210.
- van der Veen, I., de Boer, J., 2012. Phosphorus flame retardants: properties, production, environmental occurrence, toxicity and analysis. *Chemosphere* 88, 1119–1153.
- Vousden, K.H., Lane, D.P., 2007. p53 in health and disease. *Nat. Rev. Mol. Cell. Biol.* 8, 275–283.
- Wu, G.S., Robertson, D.H., Brooks, C.L., Vieth, M., 2003. Detailed analysis of grid-based molecular docking: a case study of CDOCKER-A CHARMM-based MD docking algorithm. *J. Comput. Chem.* 24, 1549–1562.
- Zhang, G.W., Wang, L.H., Zhou, X.Y., Li, Y., Gong, D., 2014. Binding characteristics of sodium saccharin with calf thymus DNA *in vitro*. *J. Agric. Food Chem.* 62, 991–1000.
- Zhao, L., Yao, Y.C., Li, S., Lv, M.J., Chen, H., Li, X.L., 2014. Cytotoxicity and DNA binding property of triphenylethylenecoumarin hybrids with two amino side chains. *Bioorg. Med. Chem. Lett.* 24, 900–904.
- Zhu, J.H., Chen, L.L., Dong, Y.Y., Li, J.Z., Liu, X.H., 2014. Spectroscopic and molecular modeling methods to investigate the interaction between 5-hydroxymethyl-2-furfural and calf thymus DNA using ethidium bromide as a probe. *Spectrochim. Acta. A* 124, 78–83.